IOPscience

HOME | SEARCH | PACS & MSC | JOURNALS | ABOUT | CONTACT US

Dynamical screening and carrier mobility in GaAs-GaAlAs heterostructures

This article has been downloaded from IOPscience. Please scroll down to see the full text article.

1985 J. Phys. C: Solid State Phys. 18 L593

(http://iopscience.iop.org/0022-3719/18/20/005)

The Table of Contents and more related content is available

Download details:
IP Address: 129.8.242.67
The article was downloaded on 30/09/2009 at 06:13

Please note that terms and conditions apply.

J. Phys. C: Solid State Phys. **18** (1985) L593–L597. Printed in Great Britain

LETTER TO THE EDITOR

Dynamical screening and carrier mobility in GaAs–GaAlAs heterostructures

X L Lei
Department of Physics, City College of New York, New York, NY 10031, USA
and Shanghai Institute of Metallurgy, Chinese Academy of Sciences, Shanghai, China

Received 1 May 1985

Abstract. The ohmic mobility due to acoustic and polar optical phonon scattering in a GaAs–GaAlAs heterojunction is calculated by the use of a formula in which temperature, wave vector and frequency-dependent screening is built in. It is shown that under RPA the enhancement of the polar optical phonon-induced resistivity due to dynamical effects almost compensates the reduction by static screening over the entire temperature region.

Recently there has been considerable interest in the effect of free-carrier screening on polar optical phonon interaction in GaAs–GaAlAs heterostructures (Price 1981, Das Sarma and Mason 1985, Lyon and Yang 1985, Lei *et al* 1985). The earliest discussion on carrier screening in this system was given by Price (1981). In most later mobility calculations, however, the carrier screening effects were considered only within the long wave and static approximation (Debye model) for impurity and acoustic phonon scattering or completely neglected for polar optical phonon scattering until very recent investigations emerged. Das Sarma and Mason (1985) calculated the imaginary part of the polaron self-energy (called polar scatering rate) using the static RPA for screening. They found that screening substantially reduces (by as much as a factor of ten) the polar scattering rate, thus calling into question most of the theoretical work done where the screening is ignored. At the same time Lyon and Yang (1985) calculated the polar optical phonon scattering rate using the zero-temperature but wave vector- and frequency-dependent RPA dielectric function given by Stern (1967), finding a big increase in phonon emission rate for electrons with energy higher than the energy of the longitudinal optical phonon. Unfortunately little conclusion on mobility can be drawn directly from the results of the above two groups.

The purpose of this Letter is to calculate the mobilities due to acoustic and polar optical phonon scattering in GaAs–GaAlAs heterostructures including full temperature-, wave vector, and frequency-dependent screening under RPA by a balance equation approach recently developed by Lei *et al* (1985). The electron–electron interaction, and thus the free-carrier screening, is fundamentally built into their balance equations. The linearisation of the balance equations leads to the expression for ohmic resistivity due

0022-3719/85/200593 + 05 $02.25 © 1985 The Institute of Physics

to phonons:

$$R_L = -\frac{2\hbar}{N^2 e^2 k_B T} \sum_{q,q_z,\lambda} q_\chi^2 |M(\boldsymbol{Q},\lambda)|^2 \sum_{n',n} |I_{n'n}(\mathrm{i}q_z)|^2 \times \mathrm{Im}[\hat{\Pi}(n', n, \boldsymbol{q}, \Omega_{Q\lambda})]\left[-n'\left(\frac{\hbar\Omega_{Q\lambda}}{k_B T}\right)\right]. \tag{1}$$

Here T is temperature, N is the total number of carriers per unit area, $n(x/T) = 1/[\exp(x/T) - 1]$ is the Bose function, and $M(\boldsymbol{Q}, \lambda)$ represents the matrix element in 3D plane wave representation of the interaction between electrons and the λth branch phonons with wave vector $\boldsymbol{Q}$ and frequency $\Omega_{Q\lambda}$, $\boldsymbol{Q} \equiv (\boldsymbol{q}, q_z)$. In equation (1),

$$I_{n'n}(\mathrm{i}q_z) = \int_0^\infty \exp(-\mathrm{i}q_z z)\zeta_{n'}^*(z)\zeta_n(z)\,\mathrm{d}z \tag{2}$$

is the form factor for the sub-band $n \rightarrow n'$ transition, $\zeta_n(z)$ is the envelope function of sub-band n, and $\hat{\Pi}(n', n, \boldsymbol{q}, \Omega)$ is the density–density correlation function for electrons in sub-bands n and n'. Calculating in the spirit of the random phase approximation, we obtain

$$\hat{\Pi}(n', n', \boldsymbol{q}, \Omega) = \Pi(n', n, \boldsymbol{q}, \Omega) + \Pi(n', n, \boldsymbol{q}, \Omega) \times \sum_{m',m} V_{n'n,m'm}(q)\hat{\Pi}(m', m, \boldsymbol{q}, \Omega) \tag{3}$$

in which

$$\Pi(n', n, \boldsymbol{q}, \Omega) = 2\sum_k \frac{f(E_{n'k+q}) - f(E_{nk})}{\hbar\Omega + E_{n'k+q} - E_{nk} + \mathrm{i}\delta} \tag{4}$$

is the electron density–density correlation function in the absence of intercarrier interaction. In equation (4) $E_{nk} = E_n + \hbar^2 k^2/2m$ is the energy of electron with 2D wave vector $\boldsymbol{k}$ in sub-band n and $f(E) = \{\exp[(E - E_F)/k_B T + 1]\}^{-1}$ is the Fermi function where E_F is the temperature-dependent Fermi energy, which is to be determined from the total number density N by

$$2\sum_{n,k} f(E_{nk}) = N. \tag{5}$$

In equation (3)

$$V_{m'm,n'n}(q) = \frac{e^2}{2\varepsilon_0 \kappa q} H_{m'm,n'n}(q) \tag{6}$$

with

$$H_{m'm,n'n}(q) = \int \mathrm{d}z_1\,\mathrm{d}z_2\,\zeta_{m'}^*(z_1)\zeta_m(z_1)\zeta_{n'}^*(z_2)\zeta_n(z_2)\exp(-q|z_1 - z_2|). \tag{7}$$

The contributions from image charges are neglected due to the small difference of the dielectric constants on both sides of the GaAs–GaAlAs interface. Here κ is the low-frequency dielectric constant of GaAs.

The full dynamical and temperature- and wave vector-dependent screening is included in the electron density–density correlation function $\hat{\Pi}(n', n, \boldsymbol{q}, \Omega)$.

Using $\Pi(n', n, \boldsymbol{q}, \Omega)$ (equation (4)) instead of $\hat{\Pi}(n', n, \boldsymbol{q}, \Omega)$ in equation (1), we

obtain the resistivity without the free carrier screening. On the other hand, using

$$\hat{\Pi}(n', n, q, \Omega) = \Pi(n', n, q, \Omega) + \Pi(n', n, q, 0) \sum_{m', m} V_{n'n,m'm}(q)\hat{\Pi}(m', m, q, \Omega) \tag{8}$$

for $\hat{\Pi}(n', n, q, \Omega)$ in equation (1) amounts to taking only static (but wave vector- and temperature-dependent) screening into account.

Since the acoustic phonon frequency $\Omega_Q = v_s Q$ and the sound velocity $v_s \ll$ Fermi velocity of the 2D electron for usual carrier density, the dynamical effect gives generally a small correction to the acoustic phonon-limited mobility obtained by including static screening. The optical phonon energy $\hbar\Omega_0 = 3.54$ meV, however, is usually substantially larger than the 0 K Fermi energy (measured from the lowest sub-band bottom), and so plasma resonance is appreciable for optical phonon scattering. It may significantly enhance the resistivity above the prediction value by static screening.

To obtain results applicable to room temperature, we consider two sub-bands, choosing the Fang–Howard–Stern variational functions

$$\zeta_0(z) = (b_0^3/2)^{1/2} \zeta \exp(-b_0 z/2) \tag{9}$$

and

$$\zeta_1(z) = [\tfrac{3}{2} b_1^5/(b_0^2 - b_0 b_1 + b_1^2)]^{1/2} z[1 - (b_0 + b_1)/6] \exp(-b_1 z/2) \tag{10}$$

as the envelope wave functions for the $n = 0$ and 1 sub-bands respectively. The parameters b_0 and b_1 are determined by minimising the energies E_0 and E_1 as usual.

In this way we have calculated the resistivities R_a and R_p due to acoustic phonon scattering (via piezoelectric and deformation potential interactions) and due to polar optical phonon scattering (via Frölich interaction) respectively as functions of temperature from 5 K to 300 K, taking full account of dynamical and temperature- and wave vector-dependent screening. For comparison we also calculated resistivities due to acoustic and polar optical phonon scattering, including static (but temperature- and wave vector-dependent) screening, R_{as}, R_{ps}, and without screening, R_{af}, R_{pf}, respectively.

In figure 1 we plot the ratios R_a/R_{af}, R_{as}/R_{af}, R_pR_{pf} and R_{ps}/R_{pf} as functions of temperature. Static screening reduces the resistivities in both acoustic phonon and optical phonon scatterings. As expected, in the optical phonon case the dynamical effect gives rise to a substantial enhancement of the resistivity especially at relatively low temperatures, while in the acoustic phonon case only a small correction is necessary. Strangely enough, the resistivity enhancement due to plasma resonance in the case of polar optical phonon scattering almost compensates the reduction due to static screening over the whole temperature range, making the prediction obtained by completely ignoring the carrier screening nearly correct. This might be the reason why most of the previous theoretical calculations on polar optical phonon limited mobility were in qualitative agreement with measurements.

The calculated acoustic phonon and polar optic phonon limited mobilities μ_a and μ_p are shown in figure 2, together with calculated impurity limited mobility μ_i and total mobility μ.

Impurity-induced resistivity takes the form

$$R_i = -\frac{1}{N^2 e^2} \sum_{q, n', n} q_\chi^2 |U_{n'n}(q)|^2 \frac{\partial}{\partial \Omega} [\mathrm{Im}\, \hat{\Pi}(n', n, q, \Omega)]_{\Omega=0} \tag{11}$$

for which only static screening plays a role. $U_{n'n}(q)$ here is the effective impurity scattering potential for electron transition from sub-band n to n' with momentum transfer q.

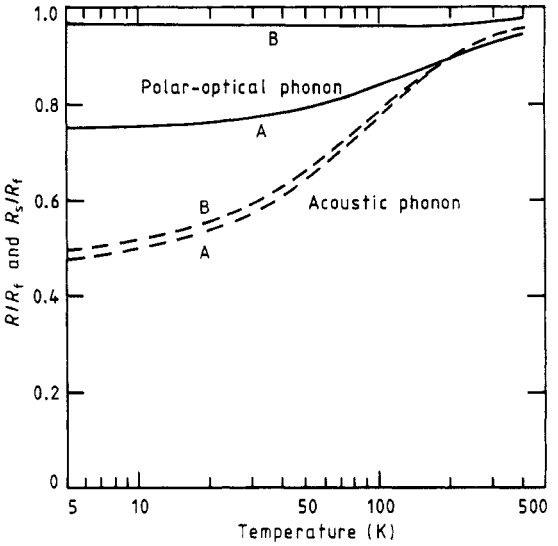

Figure 1. Ratios of the resistivities due to acoustic and polar optical phonons with dynamical or static screening to those without screening are shown as functions of temperature. Curves A, static screening (R_s/R_f); curves B, dynamical screening (R/R_f). $N = 2.2 \times 10^{11}$ cm^{-2}.

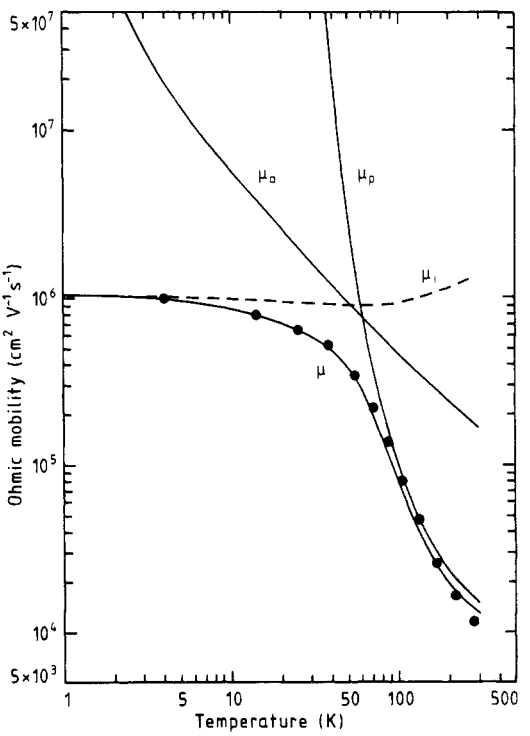

Figure 2. Polar optical phonon-, acoustic phonon- and impurity-limited ohmic mobilities μ_p, μ_a, μ_i and total mobility μ are shown as functions of temperature. The full circles are experimental data taken from Mendez *et al* (1984). $N = 2.2 \times 10^{11}$ cm^{-2}.

We consider both remote ionised dopants and background impurities, assuming equal contributions from either mechanism at zero temperature. Impurity-limited mobility decreases with increasing temperature in the low-T region, and then increases after reaching a minimum at about $T = 60$ K. This is due to the temperature variation of Fermi energy when carriers deviate from Fermi–Dirac statistics. The dots in figure 2 are the measured mobility taken from the data of Mendez *et al* (1984). The overall agreement between theoretical and experimental values is satisfying except for the highest-temperature (250–300 K) region. The material parameters used in the calculation are: density $d = 5.31$ g cm^{-3}; effective mass $m = 0.07m_e$; transverse sound velocity $v_{st} = 2.48 \times 10^3$ m s^{-1}; longitudinal sound velocity $v_{sl} = 5.29 \times 10^3$ m s^{-1}; longitudinal optical phonon energy $\hbar\Omega_0 = 35.4$ meV; low-frequency dielectric constants $\kappa = 12.9$; optical dielectric constant $\kappa_\infty = 10.8$; acoustic deformation potential $\Xi = 8.5$ eV; piezoelectric constant $e_{14} = 1.41 \times 10^9$ V m^{-1}. The remote impurities are arbitrarily assumed to be at a distance $S = 370$ Å from the interface. The only adjustable parameter is the impurity density, which is selected to match the experimental mobility at lowest temperature.

The author is indebted to J L Birman and C S Ting for helpful discussions. This work was supported by the National Science Foundation under the US–China Cooperative Science Program.

References

Das Sarma S and Mason B A 1985 *Phys. Rev.* B **31** 5536
Lei X L, Birman J L and Ting C S 1985 *Bull. Am. Phys. Soc.* **30** 590 (1985 *J. Appl. Phys.* to be published)
Lyon S A and Yang C H 1985 *Bull. Am. Phys. Soc.* **30** 208
Mendez E E, Price P J and Heiblum M 1984 *Appl. Phys. Lett.* **45** 294
Price P J 1981 *J. Vac. Sci. Technol.* **19** 599
Stern F 1967 *Phys. Rev. Lett.* **18** 546